Dynamics of greenhouse gases in the river-groundwater interface in gaining river stretch (Triffoy catchment, Belgium)

Anna Jurado[a,*], Alberto V. Borges[b], Estanislao Pujades[c], Pierre Briers[d], Olha Nikolenko[d], Alain Dassargues[d], Serge Brouyère[d]

[a] Institute for Groundwater Management, Technische Universität Dresden, Dresden, Germany

[b] Chemical Oceanography Unit, University of Liège, Liège, Belgium

[c] Department of Computational Hydrosystems, UFZ - Helmholtz Centre for Environmental Research, Leipzig, Germany

[d] University of Liège, Urban & Environmental Engineering, Hydrogeology and Environmental Geology, Aquapôle, Liège, Belgium

* *Corresponding author: Anna Jurado Tel.: +49 351-463-44167 Fax: +49-3501-530022*

E-mail address: annajuradoelices@gmail.com / anna.jurado@tu-dresden.de

Current Postal address: Pratzschwitzer Str. 15, 01796 Pirna, Germany

Abstract

This study investigates the occurrence of greenhouse gases (GHGs) and the role of groundwater as an indirect pathway of GHG emissions into surface waters in a gaining stretch of the Triffoy River agricultural catchment (Belgium). To this end, nitrous oxide (N_2O), methane (CH_4) and carbon dioxide (CO_2) concentrations, the stable isotopes of nitrate and major ions were monitored in river and groundwater during 8 months. Results indicated that groundwater was strongly oversaturated in N_2O and CO_2 with respect to atmospheric equilibrium (50.1 vs. 0.55 µg/L for N_2O and 14,569 vs. 400 ppm for CO_2), but only marginally for CH_4 (0.45 vs. 0.056 µg/L), suggesting that groundwater can be a source of these GHGs to the atmosphere. Nitrification seemed to be the main process for the accumulation of N_2O in groundwater. Oxic conditions prevailing in the aquifer were not prone to the accumulation of CH_4. In fact, the emissions of CH_4 from the river were one to two orders of magnitude higher than the inputs from groundwater, meaning that CH_4 emissions from the river were due to CH_4 in-situ production in river-bed or riparian zone sediments. For CO_2 and N_2O, average emissions from groundwater were 1.5×10^5 kg CO_2 Ha^{-1} y^{-1} and 207.1 kg N_2O Ha^{-1} y^{-1}, respectively. Groundwater is probably an important source of N_2O and CO_2 in gaining streams but when the measures are scaled at catchment scale, these fluxes are probably relatively modest. Nevertheless, their quantification would better constrain nitrogen and carbon budgets in natural systems.

Keywords: Greenhouse gases, indirect emissions, river-groundwater interface, gaining stream, field scale, Belgium

1. Introduction

Anthropogenic application of organic and inorganic fertilisers of nitrogen (N) in agricultural landscapes and livestock wastes have a negative impact on groundwater resources quality due to leaching of N species into aquifers (Glavan et al., 2017). Agricultural practices represented up to one third of anthropogenic emissions of greenhouse gases (GHGs) (Gilbert, 2012), such as nitrous oxide (N_2O), methane (CH_4) and carbon dioxide (CO_2), which all contribute to climate change and N_2O to stratospheric ozone destruction (IPCC, 2014). Therefore, aquifers below agricultural landscapes can be an indirect source of GHG emissions to the atmosphere because groundwater is generally oversaturated in these GHGs with respect to atmospheric equilibrium (Bell et al., 2017; Jurado et al., 2018; McAleer et al., 2017).

Dynamics of GHGs in groundwater are complex because their occurrence depends on the geochemical conditions (e.g., nitrate NO_3^-, ammonium NH_4^+, dissolved oxygen DO, organic carbon OC, bicarbonate HCO_3^-, pH, among others) that control nitrogen (N) and carbon (C) cycles (Nikolenko et al., 2018; Jahangir et al., 2013). Denitrification is considered to be the main process of NO_3^- attenuation under anaerobic conditions in groundwater but N_2O is an intermediate product (Rivett et al., 2008). When NO_3^- is non-limiting and at intermediate DO concentrations, N_2O is not reduced to N_2 and it can accumulate in shallow groundwater (Deurer et al., 2008). Nitrification also contributes to the N_2O production in groundwater, in which case N_2O is a byproduct that can be produced during the oxidation of nitrite (NO_2^-) to NO_3^- (e.g., Vilain et al., 2012). In addition, hydrogeological parameters (e.g., groundwater table, rainfall periods and aquifer permeability) also play a major role on the dynamics of N_2O in groundwater (Jahangir et al., 2013). For instance, Deurer et al. (2008) suggested that during high-intensity precipitation events, denitrification might be inhibited in the Fuhrberger Feld aquifer (Germany) by the transport of DO with the infiltrating water. This situation promoted variable geochemical conditions leading to “cold” and ‘hot” spots of N_2O in near surface

groundwater. Concerning C species, the presence of CH_4 in shallow groundwater is associated with strongly anaerobic environments such as wetlands and landfills and comes from a biogenic origin (Bell et al., 2017). For example, Cheung et al. (2010) reported that dissolved CH_4 in shallow groundwater of Alberta (Canada) was of biogenic origin via CO_2 reduction. Likewise, CO_2 is also produced and consumed by several processes in groundwater, such as plant root respiration, oxidation of organic matter and the precipitation and dissolution of carbonate minerals (Wang et al., 2015).

Several studies have assessed the indirect GHG emissions in aquifers below agricultural landscapes (Hasegawa et al., 2000; Jahangir et al., 2012; McAleer et al., 2017; Minamikawa et al., 2010; Vilain et al., 2012; von der Heide et al., 2009) but the contribution of groundwater as a source of GHGs via surface water bodies such as streams and rivers has received less attention. Groundwater discharge to river (base flow) has been recognized as a potential pathway of N_2O into streams and rivers, which generally are net sources of N_2O in N rich environments (Beaulieu et al., 2012; Fox et al., 2014, Gardner et al., 2016; Werner et al., 2012) but can be sinks of N_2O in N and DO poor environments (Borges et al. 2015; 2018). Groundwater has also been recognised as an important source of CO_2 in riverine systems (Worral and Lancaster, 2005), especially in small streams and headwaters (Hotchkiss et al., 2015, Johnson et al., 2008). Recently, Borges et al. (2018) have reported that surface waters of the Meuse River network (Belgium) act as a source of CO_2, CH_4 and N_2O to the atmosphere. The authors pointed out that the extremely high concentrations of N_2O and CO_2 in groundwater might indicate that part of these GHGs could come from groundwater in the Meuse basin, although the actual fraction remains to be quantified.

To date, studies that have simultaneously quantified the contribution of groundwater as a potential source of N_2O, CH_4 and CO_2 in rivers are scarce. Moreover, several authors have recently stated that groundwater-surface water interactions and groundwater hydrology

require further analysis to better estimate the contribution of GHGs dissolved in groundwater into atmospheric fluxes at a local scale (Hinshaw and Dahlgren, 2016; Jurado et al., 2018; Vidon and Serchan, 2016). The objectives of this study are to (1) investigate the occurrence and examine the sources of GHGs in the river-groundwater interface and (2) evaluate the contribution of indirect GHG emissions from groundwater into surface waters. To this end, GHGs, major and minor ions and stable isotopes were sampled over 8 months in a small river catchment (Triffoy) located in the Walloon Region (Belgium).

2. Materials and methods

2.1 Study area

The Triffoy River catchment, with an area of 30.31 km^2, is in the natural region of Condroz in Wallonia (Belgium) (Fig. 1). It is an agricultural catchment where land use is dominated by cropland (48%) and grassland (38%). The remaining territory is occupied by urban areas (7%), forests (6%) and natural environments (1%). There are no industries in the whole catchment but NO_3^- concentrations can exceed the limit of good status during winter due to leaching of agricultural soil NO_3^- residue by infiltrating water (Brouyère et al., 2015; 2017). The climate is oceanic temperate, with an average annual rainfall of 900 mm and an average annual temperature of 10 ºC.

The Triffoy River intersects geological formations of Palaeozoic age, from Devonian to Carboniferous (Briers et al., 2016a). It flows through a Carboniferous limestone syncline located between two Frasnian-Famennian sandstone crests. At the base of Carboniferous limestone, the Hastarien shales constitute impermeable hydrogeological barriers separating the Carboniferous limestone aquifer from the Famennian sandstone aquifer. The sandstone aquifer is limited in extension and capacity. In contrast, the Carboniferous limestone aquifer is

120 an important groundwater reservoir that belongs to one of the most productive groundwater
121 bodies of Wallonia (RWM21, Fig.1). The limestone aquifer is exploited by two water
122 catchments: Jamagne (2,600,000 $m^3 y^{-1}$) and the Compagnie Intercommunale Liégeoise des
123 Eaux (CILE, 700,000 $m^3 y^{-1}$).

124 Previous studies carried out in this basin reported two different types of river-groundwater
125 interactions (Briers et al., 2016b): (i) gaining streams where water level is higher in the
126 groundwater, feeding river and helping to maintain its base flow and (2) losing streams where
127 river water recharges the aquifer. The stretch of river monitored in this study is a gaining
128 stream (Fig. 1) and therefore it is suitable to quantify the groundwater contribution to GHGs
129 emissions from rivers. On average, it was estimated that 92% of the Triffoy River baseflow
130 comes from groundwater recharge (Briers et al., 2016c).

131 A river segment of 2 Km (from Jamagne to State river sampling locations, Fig.1) was
132 monitored over 8 months using river gauging and pressiometric and temperature probes
133 installed in piezometers and in the river (MPZ river sampling location, Fig. 1). The
134 monitoring network for the analysis of GHGs is composed by 3 river sampling locations
135 (Jamagne, MPZ and State) and 7 groundwater observation points: 5 shallow piezometers
136 (MP-4, MP2-3, MP2-6, MP3-3 and MP3-6) and two springs (S1 and S2). The location of
137 these points and the characteristics of the piezometers are summarized in Figure A and Table
138 A (supplementary material).

139 **2.2 Groundwater and river sampling**

140 A total of six field campaigns were carried out from October 2016 to May 2017 (October
141 (C1) and December (C2) 2016 and January (C3), February (C4), March (C5) and May (C6)
142 2017). Forty samples were collected from groundwater and 18 from the Triffoy River at
143 different locations (Fig. 1). Before sampling, the piezometers were purged by pumping three

144 well volumes to remove the stagnant water and samples were collected when field parameters
145 were stabilised. Temperature (°C), electrical conductivity (EC, µS/cm), pH and DO (mg/L)
146 were measured with a portable multi-probe (YSI 556 MPS) within a flow-through cell.
147 Samples were stored in a field refrigerator and taken to the laboratory at the end of the
148 sampling day.

149 Groundwater samples were collected through tubing avoiding any contact with the
150 atmosphere. Sampling in surface waters was carried out using a 1.7 L Niskin bottle (General
151 Oceanics). Samples for CH_4 and N_2O were transferred with tubing from the Niskin bottle to
152 50 ml borosilicate serum bottles that were poisoned with a saturated solution of $HgCl_2$ (200
153 µl), sealed with a butyl stopper and crimped with an aluminum cap. Four polypropylene
154 syringes of 60 ml for measurements of pCO_2 were filled from each sampling point. For the
155 general chemistry (major and minor ions), groundwater samples were collected in
156 polypropylene bottles of 180 mL for major and minor ions and 125 mL for metals (iron (Fe)
157 and manganese (Mn)). Metal samples were filtered through a 0.45 µm polyethersulphone and
158 micro-quartz fibre filter and acidified with 1 mL of HCl 12N for sample preservation.
159 Samples for NO_3^- isotopes were collected in polypropylene bottle of 60 mL and filtered
160 through 0.22 µm nylon filter. Samples to determine dissolved organic carbon (DOC) were
161 filtered through 0.22 µm nylon filter and stored in 40 ml borosilicate vials with
162 polytetrafluoroethylene (PTFE) coated septa and poisoned with 100 µL of H_3PO_4 (85%).

163 **2.3 Analytical methods**

164 The dissolved concentrations of N_2O and CH_4 were analysed with the headspace
165 equilibration technique (25 mL of N_2 headspace in 50 mL serum bottles) and measured by gas
166 chromatography (GC) fitted with electron capture detection (ECD, SRI 8610C) for N_2O and
167 flame ionization detection (FID) for CH_4. The SRI 8610C GC-ECD-FID was calibrated with
168 certified CH_4:CO_2:N_2O:N_2 mixtures (Air Liquide Belgium) of 0.2, 2 and 6 ppm N_2O and of 1,

10 and 30 ppm CH_4. The pCO_2 was measured in the field using an infrared gas analyser (Li-Cor Li-840) a few minutes after sampling by creating a headspace with ambient air in the polypropylene syringes (1:1 ratio of air and water) (Abril et al., 2015). The Li-840 was calibrated with a suite of CO_2:N_2 mixtures (Air Liquide Belgium) with mixing ratios of 388, 813, 3,788, 8,300 and 19,150 ppm CO_2. The reproducibility of the measurements was ±3.2%, ±3.9% and ±2.0% for N_2O, CH_4 and pCO_2, respectively. Major ions (Na^+, Mg^{2+}, K^+, Cl^-, SO_4^{2-} and NO_3^-) and minor ions (NO_2^- and NH_4^+) were measured by ion chromatography via a specific ion exchange resin and a conductivity detector. Calcium (Ca^{2+}) concentrations and alkalinity were obtained by potentiometric titration in the laboratory. Fe and Mn concentrations were obtained by atomic absorption spectrometry. Nitrogen ($\delta^{15}N_{NO3}$) and oxygen ($\delta^{18}O_{NO3}$) isotope analyses of NO_3^- were determined by a mass DELTA V plus spectrometer plus a GasBench II from Thermo using the denitrifier method that convert all sampled NO_3^- to N_2O (Sigman et al., 2001; Casciotti et al., 2002). The notation was expressed in terms of delta (δ) per mil (‰) relative to the international standards for the environmental isotopes (V-SMOW for $\delta^{18}O$ and AIR-N_2 for $\delta^{15}N$ of NO_3^-). The reproducibility of NO_3^- isotope samples was ±0.4‰ for $\delta^{15}N$ and ±1.6‰ for $\delta^{18}O$ of NO_3^-. The NO_3^- isotope results represent the mean value of true double measurements of each sample. DOC concentration was determined with a wet oxidation total organic carbon analyser (IO Analytical Aurora 1030 W) coupled with an EA-IRMS (ThermoFinnigan DeltaV Advantage).

2.4 Indirect greenhouse gas emissions from groundwater

The indirect GHG emissions from groundwater to the river ($E_{GHG\text{-}Gw}$) were evaluated using hydrogeological data and the dissolved concentrations of GHGs measured in the groundwater as follows:

$$E_{GHG-Gw} = \frac{Q_{dis} \times \left[C_{GHG-Gw} - C_{GHG-Eq} \right]}{A} \quad (1)$$

193 where Q_{dis} is groundwater discharge into the Triffoy River (m^3 d^{-1}), $C_{GHG\text{-}Gw}$ is the measured
194 concentration of a given GHG in groundwater observation points (µg/L), $C_{GHG\text{-}Eq}$ is the GHGs
195 air-equilibrated water concentration and A is the area of the river between the upstream and
196 the downstream river sampling locations (0.51 Ha). Groundwater discharge into the Triffoy
197 River (Q_{dis}) was estimated by the difference in stream flow rate between the upstream
198 (Jamagne, Q_{in}) and the downstream (State, Q_{out}) river sampling locations (Fig. 1). Note that
199 groundwater was considered the only recharge source of the river because baseflow
200 conditions prevailed during all the monitoring period. Hence, *Eq. (1)* represents the maximal
201 flux of GHGs from groundwater to the river.
202 The fluxes of GHGs from groundwater to the river (*Eq. (1)*) were compared with those from
203 the river surface to the atmosphere ($E_{GHG\text{-}Riv}$). The latter were computed according to:

204 $$E_{GHG-Riv} = k \text{ x } \Delta G = k \text{ x} \left[C_{GHG-Riv} - C_{GHG-Eq} \right] \quad (2)$$

205 where k is the gas transfer velocity and ΔG is the air-water gradient (Δ) of a given gas (G).
206 The air water gradient is difference between the measured concentration of a given GHG in
207 river water ($C_{GHG\text{-}Riv}$, µg/L) and the GHG air-equilibrated water concentration ($C_{GHG\text{-}Eq}$,
208 µg/L). k was calculated from the gas transfer velocity normalised to a Schmidt number of 600
209 ($k600$) with the Schmidt numbers of N_2O, CH_4 and CO_2, computed from in-situ water
210 temperature according to Wanniknhof (1992). k_{600} (cm h^{-1}) was computed with the
211 parameterisation of Raymond et al. (2012) as a function of stream velocity (v in m s^{-1}) and
212 slope of the river channel (S is 0.0135, unitless):

213 $$k_{600} = 2.02 + 2841 \text{ x } v \text{ x } S \quad (3)$$

214 This parameterisation was derived from a compilation of gas tracer experiments in small to
215 medium sized rivers and streams, and is then adequate to compute k_{600} in the Triffoy River.

Note that the fluxes computed using *Eq. (1)* and *Eq. (2)* should be similar if groundwater is the only source of GHGs to the river (i.e., there are no processes that consumed or produced these GHGs in the river-groundwater interface).

Finally, the indirect groundwater N_2O emissions were also estimated at catchment scale using the Intergovernmental Panel on Climate Change methodology (IPCC, 2006) as follows:

$$E_{N_2O-GW} = 0.3\ \text{NLeach x}\ EF_{5g} = 0.3\text{NLeach x}\ \frac{c\,N_2O-N}{c\,NO_3^- - N} \qquad (4)$$

This method considers that 30% of fertiliser and manure N applied to soils in agricultural areas is leached to groundwater (NLeach). The EF_{5g} is the emission factor from groundwater and it is defined as the mass ratio of the dissolved concentrations of N_2O (cN_2O-N) and NO_3^- ($cNO_3^- - N$) in groundwater.

3. Results and discussion

3.1 Climatic conditions, water levels and groundwater discharge

Data regarding weather conditions and water levels help to understand the water dynamics in the river-groundwater interface. Figure 2 shows rainfall (mm), temperature (°C) and water levels (in meters above the sea level, m.a.s.l.) from December 2016 to May 2017. Total rainfall was 311 mm from October 2016 to May 2017. This value is low compared to the average monthly precipitation for the period 2012-2015 (311 mm vs. 561.4 mm; Table B, supplementary material). All sampled months, except March, presented a lower amount of precipitation than the previous years. The driest months were April 2017 and December 2016 with total precipitations of 15.7 mm and 21.4 mm, respectively (Fig. 2a). In December 2016, the amount of precipitation was 5 times lower than the average monthly precipitation for 2012-2015 (21.4 mm vs. 98.4 mm). Conversely, November was a relatively wet month with

60 mm of precipitation. During the studied period, daily air temperature ranged from -9°C (January 2017) to 19.6°C (March 2017) with an average value of 4.5°C (Fig. 2b). Diurnal air temperature variation turned out to be large. In contrast, the temperatures of river water and, especially, of groundwater were more constant. Groundwater temperatures ranged from 7.9°C to 9°C with an average temperature of 8.2°C. River water temperatures varied from 2.3°C to 12.8°C with an average temperature of 7.9°C, which was similar to the average groundwater temperature.

Figure 2c shows the evolution of water levels (m.a.s.l.) in the river (MPZ sampling location) and in groundwater (piezometers MP-4, MP2-6 and MP3-6). River and groundwater levels were relatively constant during the sampling period. Water levels slightly increased from January to March 2017 after rain events and progressively decreased due to scarce rain occurred in April and May. It is also important to point out that river water level was always lower than those of groundwater, indicating a continuous groundwater discharge to the river. This observation is also supported by temperature measured in the river because it followed the same pattern than groundwater temperature although it was also partly influenced by air temperature (Fig. 2b).

As pointed out before, groundwater was considered the only source of recharge to the Triffoy River (i.e., 100% groundwater) and the contribution of runoff was likely to be insignificant due to the scarce rain events occurred during the sampling period (Fig. 2a). The average groundwater discharge for the sampling period was 5,870±1,310 m^3 d^{-1} and it was higher during the colder months (January and March, being 7,450 m^3 d^{-1} and 7,040 m^3 d^{-1}) compared to the most temperate ones (May 2017 being 3,840 m^3 d^{-1}).

3.2 Hydrochemistry of the Triffoy River basin

3.2.1 General hydrochemistry

263 Understanding the interactions between groundwater and surface water is a key issue to
264 quantify the contribution of groundwater as an indirect source of GHGs via rivers, especially
265 in gaining rivers where groundwater is the main source of river recharge. Figure 3 shows the
266 average concentrations for major ions, metals, redox indicators and GHGs in the Triffoy River
267 versus the average concentrations in the aquifer from October 2016 to May 2017. It can be
268 observed that major ions presented similar concentrations in the river and in the aquifer,
269 indicating that groundwater clearly controlled the chemical composition of the Triffoy River.
270 The hydrochemical conditions of groundwater and river water are described using the in-
271 situ parameters measured in the field and major ions (Table 1 and Fig. 4). Groundwater pH
272 values ranged from 7 to 7.8 (average is 7.4±0.2). River pH values were slightly higher than
273 those from groundwater with an average value of 8.0±0.2. Average EC values were similar in
274 groundwater and river water being 673±35 µS/cm and 665±53 µS/cm, respectively.
275 Groundwater concentrations of DO and DOC displayed lower values than river water (Table
276 1, Fig. 3). Averages DO and DOC concentrations were 4.8±1 mg/L and 0.94±0.47 mg/L in
277 groundwater and 9.2±1.1 mg/L and 1.4±0.70 mg/L in the river.
278 Major ion compositions showed that groundwater and river water were of Ca-(Mg)-HCO_3
279 type accounting for all sampling campaigns (see Fig. B of the supplementary material). The
280 range and average concentrations and standard deviations for bicarbonate (HCO_3^-), Ca^{2+},
281 Mg^{2+} and NO_3^- for the groundwater observation points and the three river locations are shown
282 in Table 1. Note that NH_4^+ concentrations are not included because they were below detection
283 limit. The concentrations of these tracers did not present large variation neither spatially nor
284 temporarily in groundwater and river water samples (Fig. 4 and Table C of the supplementary
285 material). For instance, average NO_3^- concentrations ranged from 18.6 mg/L to 22.4 mg/L and
286 average HCO_3^- concentrations ranged from 353.3 mg/L to 361.7 mg/L in groundwater (Table
287 C of the supplementary material).

3.2.2 Occurrence of greenhouse gases

Average GHG concentrations in groundwater and river water are summarized in Table 1. Groundwater was largely oversaturated in N_2O and pCO_2 whilst only slightly oversaturated in CH_4 compared with the atmospheric equilibration concentrations (0.55 µg/L for N_2O, 400 ppm for CO_2 and 0.056 µg/L for CH_4). N_2O concentrations ranged from 26 µg/L to 87.6 µg/L (average concentration of 50.1±16.7 µg/L), CH_4 concentrations ranged from 0.01 µg/L to 4.8 µg/L (average concentration of 0.45±0.89 µg/L) and pCO_2 values varied from 8,285 to 21,897 ppm (average of 14,569±3,843 ppm). Average N_2O concentrations in groundwater were higher in temperate months (October 2016 and May 2017 being 55.2 µg/L and 54.1 µg/L, respectively) than in winter months (minimum average concentration was 46.1 µg/L in January 2017) (Table C of the supplementary material). Average pCO_2 concentrations were constant from October 2016 to February 2017 (around 14,200 ppm) and the highest value was detected in May 2017 (15,402 ppm) (Table C of supplementary material).

Average GHG concentrations in river water were 10±6.3 µg/L for N_2O, 6.9±16.6 µg/L for CH_4 and 3,168±1,253 ppm for pCO_2. The concentrations of N_2O and pCO_2 in groundwater were systematically higher than those found in river water (Fig. 3 and Fig. 4b and 4d). On the contrary, dissolved CH_4 concentrations were lower in groundwater than in the river (average concentrations were 0.45±0.89 µg/L vs. 6.9±16.6 µg/L, respectively). This observation shows that groundwater was not a source of CH_4, as also concluded by Borges et al. (2018) based on large scale analysis in the Meuse basin in Wallonia.

3.2.3 Stable isotopes

Figure 5 shows $\delta^{15}N_{NO3} - \delta^{18}O_{NO3}$ compositions for the groundwater (black dots) and river samples (grey dots) and boxes representing the isotopic compositions of possible NO_3^- sources (Kendall, 1998, Mayer, 2005). The isotopic compositions for $\delta^{15}N_{NO3}$ varied from +4.9‰ to +7.3‰ (average composition +6‰±0.57) for groundwater samples and from

+6.2‰ to +9.9‰ (average composition +7.5‰±0.85) for river samples. The isotopic compositions for $\delta^{18}O_{NO3}$ ranged from +1.1‰ to +6.8‰ (average composition +2.9‰±1.7) for groundwater samples and from +1.9‰ to +6.9‰ (average composition +3.3‰±1.5) for river samples. All groundwater and river samples agreed with the isotopic values of organic N from soil and/or the lightest values of $\delta^{15}N_{NO3}$ coming from manure or sewage water.

3.3 Processes that produce and/or consume greenhouse gases in groundwater

Nitrous oxide

The occurrence of N_2O depends on geochemical conditions prevailing in groundwater. Oxic conditions observed in groundwater might indicate that N_2O resulted from nitrification rather than denitrification since the latter is generally associated with low concentrations of DO. The positive correlation between NO_3^- and N_2O (r=0.62, Fig. C1 of the supplementary material) also suggests that nitrification was the main process for the accumulation of N_2O in groundwater. Such positive correlation was also observed in other aquifers located below agricultural catchments where nitrification was the main N_2O production mechanism (Gardner et al., 2016; Hisckok et al., 2003; Vilain et al., 2012). In addition, the positive correlation between Cl^- (conservative tracer) and NO_3^- (r=0.96, Fig. C2 of the supplementary material) might indicate that NO_3^- was not affected by denitrification because their concentrations remained constant during the sampling campaigns (Fig. 4a and 4c).

The values of NO_3^- stable isotopes also suggest N_2O was produced by nitrification because all groundwater samples fell in the box of soil N (Fig. 5). Values of $\delta^{15}N_{NO3}$ found in groundwater ($\delta^{15}N_{NO3}$=+6‰) are much lower than those expected from denitrification processes which usually present $\delta^{15}N_{NO3}$>+15‰ (Otero et al., 2009; McAleer et al., 2016). Experimental studies (e.g., Anderson and Hooper, 1983; Mayer et al., 2001) have pointed out that $\delta^{18}O_{NO3}$ generated by nitrification can be calculated as follows:

$$\delta^{18}O_{NO3} = 2/3\ \delta^{18}O_{water} + 1/3\ \delta^{18}O_{atmos} \quad (5)$$

Eq. (5) shows that two oxygens come from water and one from atmospheric oxygen during the conversion of NH_4^+ to NO_3^-. For the Triffoy River catchment, using an isotopic value for $\delta^{18}O_{water}$ of –7.3‰ obtained from a previous study (Briers et al., 2016d) and an isotopic value for $\delta^{18}O_{atmos}$ of +23.5‰ (Kroopnick and Craig, 1972), the evaluated $\delta^{18}O_{NO3}$ is equal to +3‰. This value is very close to the average value for $\delta^{18}O_{NO3}$ observed in the collected groundwater samples (+2.9±1.7‰). Hence, N_2O found in groundwater seems to be produced due to nitrification in the unsaturated zone.

Methane

The oxic conditions that prevailed underground in the Triffoy River basin were not favourable for the accumulation of CH_4 in groundwater. The average concentration in river water was higher than those in groundwater (6.9 µg/L vs. 0.45 µg/L, Fig. 3), suggesting that groundwater was an insignificant source of CH_4 in the river.

Carbon dioxide

CO_2 enrichment in groundwater might occur when rain water percolates through the soil, where CO_2 is produced by processes such as microbial decomposition of organic matter (heterotrophic respiration) and root respiration (autotrophic respiration) (Tan, 2010), and subsequent leaching of CO_2 to groundwater. These processes produce an enrichment of CO_2 and groundwater pCO_2 values are typically between 10 to 100 times higher than atmospheric pCO_2. When the oversaturated groundwater is discharged in the Triffoy River, CO_2 degassing into the atmosphere takes place. This situation leads to an increase of pH in the river water and the progressive precipitation of carbonate minerals. In fact, average saturation indexes (SIs, see text S1 of the supplementary material) of carbonate minerals were higher in river water than in groundwater being 0.79 vs. 0.24 for calcite and 0.43 and –0.55 for dolomite,

indicating that river water was slightly oversaturated with respect to calcite and dolomite (Table D of the supplementary material).

Other processes that might produce CO_2 in groundwater are redox processes such as aerobic respiration and denitrification. Nevertheless, these processes were not likely to occur in the aquifer because of the presence of DO and NO_3^- in groundwater (see previous explanation that supports the occurrence of nitrification).

3.4 Evaluation of greenhouse gas emissions from groundwater

In this section, the importance of groundwater as an indirect source of GHGs to the atmosphere was assessed at local scale (per area of the river from Jamagne to State river sampling locations, section 3.4.1). Afterwards, to place the groundwater GHG emissions in a broader context, the resulting average emissions in section 3.4.1 were upscaled by dividing them by the total agricultural area of the Triffoy River basin (section 3.4.2).

3.4.1 Local scale

The maximal contribution of GHG emissions from groundwater to the river was assessed using *Eq. (1)*. Average GHG fluxes from groundwater resulted in 207 kg N_2O Ha^{-1} y^{-1}, 1.6 kg CH_4 Ha^{-1} y^{-1} and 1.5×10^5 kg CO_2 Ha^{-1} y^{-1}. These fluxes should be similar to those from the river to the atmosphere unless that there are other processes that consumed or produced N_2O, CH_4 and CO_2 in the river-groundwater interface. Average fluxes evaluated from river surface to the atmosphere (*Eq. (2)*) were similar to those evaluated with *Eq. (1)* for N_2O and CO_2 (126.9 kg N_2O Ha^{-1} y^{-1} and 9.7×10^4 kg CO_2 Ha^{-1} y^{-1}, respectively) but much higher for CH_4 (105 kg CH_4 Ha^{-1} y^{-1}).

Monthly flux estimates using *Eq. (1)* for N_2O ($E_{N2O\text{-}Gw}$) and CO_2 ($E_{CO2\text{-}Gw}$) were systematically higher than those computed with *Eq. (2)* ($E_{N2O\text{-}Riv}$ and $E_{CO2\text{-}Riv}$) (except for N_2O in May) (Fig. 6). This observation indicates that groundwater contributed to the emissions of these two gases to the atmosphere but part of the N_2O and CO_2 concentrations might had been

386 consumed in the river-groundwater interface. If these GHGs were not consumed before
387 reaching the river, their average concentrations should have been similar to those observed in
388 groundwater. However, groundwater concentrations for N_2O and CO_2 were 5 times higher
389 than those measured in the river (50.1 µg/L vs. 10 µg/L for N_2O and 14,569 ppm vs. 3,168
390 ppm for pCO_2). The biggest difference in N_2O and CO_2 emissions (using *Eq. (1)* and *Eq. (2)*)
391 occurred in January 2017 when groundwater discharge into the river was maximum. It is
392 important to mention that N_2O emissions from the river to the atmosphere (*Eq. (2),* $E_{N2O\text{-}Riv}$)
393 were higher than those from groundwater (*Eq. (1),* $E_{N2O\text{-}Gw}$) in May 2017 (Fig. 6). This
394 observation might be explained by the low groundwater discharge into the river compared to
395 other months (3,840 $m^3\ d^{-1}$) and the slightly higher concentration of N_2O found in river water
396 in May 2017 (Table C of the supplementary material) but also it could indicate an inflow of
397 N_2O produced in the river from upstream. The opposite situation was observed for CH_4,
398 whose emissions from the river to the atmosphere ($E_{CH4\text{-}Riv}$) were always one to two orders of
399 magnitude higher than the input of CH_4 from the groundwater ($E_{CH4\text{-}Gw}$) (Fig. 6). This implies
400 that the emission of CH_4 from the river to the atmosphere was almost exclusively sustained by
401 in-situ production most probably in river-bed sediments or riparian areas.

402 **3.4.2 Catchment scale**

403 To evaluate the GHGs emissions at catchment scale, the average $E_{GHG\text{-}Gw}$ (*Eq. (1)*) were
404 divided by the agricultural area of the Triffoy basin (26.1 km^2) instead of the surface of the
405 river ($5.1 \times 10^{-3}\ km^2$). This resulted in average fluxes of 0.040 kg $Ha^{-1}\ y^{-1}$ for N_2O, 3.0×10^{-4}
406 kg $Ha^{-1}\ y^{-1}$ for CH_4 and 29.8 kg $Ha^{-1}\ y^{-1}$ for CO_2. Note that these fluxes were evaluated
407 considering a river stretch of 2 km but the total length of the Triffoy River is 12 km (Fig. 1).

408 Indirect groundwater N_2O emissions at catchment scale were also evaluated applying the
409 IPCC method (*Eq. (4)*) that requires the evaluation of the emission factor for groundwater
410 (EF_{5g}). The EF_{5g} coefficient evaluated in this study is 3 times higher than the default value

411 proposed by the IPCC (0.0069±0.0018 vs. 0.0025). Considering that N leaching to
412 groundwater was estimated to be 5.4 kg N Ha^{-1} y^{-1} in the aquifers of the Condroz region
413 (SPW, 2010), the resulting indirect N_2O emissions from groundwater were 0.037 kg N_2O-N
414 Ha^{-1} y^{-1} (0.058 kg N_2O Ha^{-1} y^{-1}). This value is similar to the one evaluated using groundwater
415 discharge in the river (0.040 kg N_2O Ha^{-1} y^{-1}) and other N_2O fluxes from groundwater
416 evaluated in aquifers located below agricultural lands. For example, similar estimates of
417 indirect N_2O fluxes from groundwater were obtained using the IPCC methodology in the
418 Orgeval catchment in France and major UK aquifers being 0.035 kg N_2O-N Ha^{-1} and 0.04 kg
419 N_2O-N Ha^{-1} y^{-1}, respectively (Vilain et al., 2012; Hisckok et al., 2003). The IPCC approach
420 presents some limitations because N leaching to groundwater varies from one site to another.
421 For instance, Jahangir et al. (2013) reported that N leached varied from 8% to 38% of the total
422 N input in four different agricultural settings, resulting in indirect N_2O groundwater fluxes
423 ranging from 0.07 kg N_2O-N Ha^{-1} y^{-1} to 0.24 kg N_2O-N Ha^{-1} y^{-1}. Slightly lower fluxes (0.004
424 kg N_2O-N Ha^{-1} y^{-1}) were evaluated in the Choptank Basin in the USA (Gardner et al., 2016).
425 The authors pointed out that groundwater was a minor source of total biogenic N_2O emissions
426 (15% on average) from strongly gaining agricultural streams but it was the primary source of
427 N_2 (3.5 kg N_2 Ha^{-1} y^{-1}). Similarly, von der Heide et al. (2009) evaluated that N_2O fluxes from
428 the shallow groundwater of the Fuhrberger Feld aquifer (Germany) were 1 to 2 orders of
429 magnitude lower than N_2O flux at soil surface (0.044 vs. 1 kg N_2O–N Ha^{-1} y^{-1}) and thus
430 groundwater was a negligible pathway of atmospheric emissions.

431 CO_2 and CH_4 indirect fluxes from groundwater in agricultural areas have been less studied
432 than those of N_2O. For instance, Jahangir et al. (2012) evaluated the dissolved C delivery to
433 surface water through groundwater in selected agricultural aquifers of Ireland. Groundwater
434 CO_2 export was up to 314 kg C Ha^{-1} y^{-1} (1151 kg CO_2 Ha^{-1} y^{-1}) whereas CH_4 export was low
435 (from 0.013 kg CH_4 Ha^{-1} y^{-1} to 2.30 CH_4 Ha^{-1} y^{-1}). The authors concluded that the dissolved C

loss to surface waters via groundwater was not significant compared to total carbon (TC) content of the topsoil (0.06–0.18% of TC). Similarly, Wang et al. (2015) evaluated that CO_2 lost via groundwater to the stream was approximately 73 kg CO_2 Ha^{-1} y^{-1} in the Hongfeng Lake catchment (China, 1,596 km^2), which was insignificant compared with soil CO_2 emission.

To sum up, groundwater is likely to be an important source of N_2O and CO_2 in gaining streams but when measures are upscaled at the catchment-scale, these fluxes are probably relatively modest. Thus, indirect GHG emissions from groundwater seem to be a minor pathway of GHG atmospheric emissions but their quantification would help to better evaluate the C and N budgets in agricultural catchments.

4. Conclusions

As GHG concentrations have significantly increased in the atmosphere, studying their dynamics from natural systems remain a major concern. This study investigated the occurrence of N_2O, CH_4 and CO_2 and quantified the contribution of groundwater as an indirect source of these GHGs via river water in the agricultural catchment of the Triffoy River (Belgium). Average groundwater concentrations for N_2O and pCO_2 were higher than those found in the river samples (50 vs. 10 µg/L and 14569 vs. 3168 ppm, respectively), suggesting that groundwater could be an indirect source of GHGs to the atmosphere. Nitrification was likely to be the main source of N_2O in groundwater. This observation is supported by the positive relationship between N_2O and NO_3^-, the presence of DO and NO_3^- and the absence of NH_4^+ in groundwater. The oxic conditions found in groundwater were not prone for the accumulation of CH_4 in the aquifer and it might be generated in river-bed or riparian zone sediments.

The role of groundwater as an indirect source of GHGs in the river-groundwater interface was evaluated through the net groundwater discharge into the river *(Eq. (1))* and compared to the inputs from the river to the atmosphere *(Eq. (2)).* Average fluxes obtained for N_2O and CO_2 using both approaches were similar (207 vs. 126.9 kg N_2O Ha^{-1} y^{-1} and 1.5×10^5 vs. 9.7×10^4 kg CO_2 Ha^{-1} y^{-1}), showing that groundwater was a source of release of these GHGs into the atmosphere. The opposite situation was observed for CH_4, whose average emissions from groundwater were two orders of magnitude lower than those evaluated from the river to the atmosphere (1.6 vs. 105 kg CH_4 Ha^{-1} y^{-1}). This observation indicates that groundwater was an insignificant source of CH_4 to the atmosphere. Overall, groundwater in the studied gaining stream was a source that contributed to N_2O and CO_2 atmospheric emissions but when these emissions were up-scaled (from the river surface to the catchment area) the resulting fluxes seemed to be insignificant compared to other sources (i.e., direct N_2O and CO_2 emissions from soils). Nevertheless, their quantification would better constrain N and C budgets in natural systems.

We suggest that future research efforts should be devoted to investigating the dynamics of GHGs in groundwater, soil and river water over long time periods (i.e., hydrological year) and a wide range of flow conditions (wet and dry periods) to better understand the relative importance of each compartment as a source of GHGs to the atmosphere at a stream scale. Particular efforts should be directed to improve the understanding of GHGs production and consumption in the groundwater-river transition zone (e.g., streambed hyporheic sediments). This point will allow to better constrain global N_2O, CH_4 and CO_2 budgets at the river-groundwater interface and thus the N and C budgets.

Acknowledgements

A. J. and E. P. gratefully acknowledge the financial support from the University of Liège and the EU through the Marie Curie BeIPD-COFUND postdoctoral fellowship programme (2015-2017 and 2014-2016 fellows from FP7-MSCA-COFUND, 600405). This work was accomplished when A. J. and E. P. were postdoctoral researchers at the University of Liège (Belgium). A. V. B. is a senior research associate at the Fonds National de la Recherche Scientifique (FNRS). This project has received funding from the European Union's Horizon 2020 research and innovation programme under the Marie Skłodowska-Curie grant agreement No 675120. We thank Marc-Vincent Commarieu for help in gas chromatograph (GC) measurements. GC was acquired with funds from FNRS (FNRS, 2.4.598.07).

Appendix A. Supplementary material. Supplementary data associated with this article can be found in the online version.

518 **References**

519 Abril, G., Bouillon, S., Darchambeau, F., Teodoru, C. R., Marwick, T. R., Tamooh, F.,
520 Omengo, F.O., Geeraert, N., Deirmendjian, L., Polsenaere, P., Borges, A. V., 2015. Technical
521 Note: Large overestimation of pCO2 calculated from pH and alkalinity in acidic, organic-rich
522 freshwaters. Biogeosciences, 12(1), 67.

523 Andersson K. K. and Hooper A. B.,1983. O2 and H2O are each the source of one O in NO2
524 produced from NH3 by Nitrosomonas: 15N evidence. FEBS Lett. 164, 236–240.

525 Beaulieu, J.J., Tank, J.L., Hamilton, S.K., Wollheim, W.M., Hall, R.O., Mulholland, P.J.,
526 Peterson, B.J., Ashkenas, L.R., Cooper, L.W., Dahm, C.N., Dodds, W.K., Grimm, N.B.,
527 Johnson, S.L., McDowell, W.H., Poole, G.C., Valett, H.M., Arango, C.P., Bernot, M.J.,
528 Burgin, A.J., Crenshaw, C.L., Helton, A.M., Johnson, L.T., O'Brien, J.M., Potter, J.D.,
529 Sheibley, R.W., Sobota, D.J., Thomas, S.M., 2011. Nitrous oxide emission from
530 denitrification in stream and river networks. Proc. Nat. Acad. Sci. USA, 108,214–19.

531 Bell, R.A., Darling, W.G., Ward, R.S., Basava-Reddi, L., Halwa, L., Manamsa, K., Ó
532 Dochartaigh, B.E., 2017. A baseline survey of dissolved methane in aquifers of Great Britain.
533 Sci. Total Environ., 601-602, 1803-1813. doi: 10.1016/j.scitotenv.2017.05.191.

534 Borges, A. V., Darchambeau, F., Lambert, T., Bouillon, S., Morana, C., Brouyère, S.,
535 Hakoun, V., Jurado, A., Tseng, H.C., Descy, J.P., Roland, F. A. E., 2018. Effects of
536 agricultural land use on fluvial carbon dioxide, methane and nitrous oxide concentrations in a
537 large European river, the Meuse (Belgium). Sci. Total Environ., 610, 342-355.

538 Borges, A.V., Darchambeau, F., Teodoru, C.R., Marwick, T.R., Tamooh, F., Geeraert ,N.,
539 Omengo, F.O., Guérin, F., Lambert, T., Morana, C., Okuku, E., Bouillon, S., 2015. Globally
540 significant greenhouse gas emissions from African inland waters, Nature Geoscience, 8, 637-
541 642

Briers, P., Jamin, P., Ruthy, I., Orban, P., Brouyère, S., 2016a. Hydrogéologie du bassin du Hoyoux. In Atlas du Karst Wallon-Bassins versants du Hoyoux et de la Solières (pp 41-47). Service Publique de la Wallonie, Belgium.

Briers, P., Orban, P., Brouyère, S., 2016b. Caractérisation complémentaire des masses d'eau dont le bon état dépend d'interactions entre les eaux de surface et les eaux souterraines (ESO-ESU). Délivrable D3.5 Quantification des échanges nappe-rivière pour les bassins tests. Université de Liège.

Briers, P., Orban, P., Brouyère, S., 2016c. Caractérisation complémentaire des masses d'eau dont le bon état dépend d'interactions entre les eaux de surface et les eaux souterraines (ESO-ESU). Délivrable D4.1 Développement d'indicateurs des interactions entre eaux souterraines et eau de surface.

Briers, P., Orban, P., Brouyère, S., 2016d. Caractérisation complémentaire des masses d'eau dont le bon état dépend d'interactions entre les eaux de surface et les eaux souterraines (ESO-ESU). Délivrable D3.4: Caractérisation hydrochimique et campagne isotopique pour la discrimination des sources de pollution ponctuelles et diffuses du nitrate. Université de Liège.

Brouyère, S., Briers, P., Descy, J. P., Schmit, F., Degré, A., Orban, P., 2017. Convention Région wallonne et HGE-ULg Caractérisation complémentaire des masses d'eau dont le bon état dépend d'interactions entre les eaux de surface et les eaux souterraines-Délivrable D1. 8 Rapport final.

Brouyère, S., Briers, P., Schmit, F., Orban, P., Hallet, V., Delloye, F., Descy, J. P., 2015. Case study 2: Groundwater–surface water interaction in limestone areas of the GWB BE_Meuse_RWM021 (Belgium). Technical Report on Groundwater Associated Aquatic Ecosystems, 47-49.

565 Casciotti, K.L., Sigman, D.M., Hastings, M.G., Böhlke, J.K., Hilkert, A., 2002.
566 Measurement of the oxygen isotopic composition of nitrate in seawater and freshwater using
567 the denitrifier method. Analytical Chemistry 74:4905-4912.

568 Cheung, K., Klassen, P., Mayer, B., Goodarzi, F., Aravena, R., 2010. Major ion and isotope
569 geochemistry of fluids from coal bed methane and shallow groundwater wells in Alberta,
570 Canada. Appl. Geochem. 25, 1307–1329.

571 Deurer, M., von der Heide, C., Böttcher, J., Duijnisveld, W. H. M., Weymann, D., Well, R.,
572 2008. The dynamics of N_2O near the groundwater table and the transfer of N 2 O into the
573 unsaturated zone: A case study from a sandy aquifer in Germany. Catena, 72(3), 362-373.

574 Fox, R. J., Fisher, T. R., Gustafson, A. B., Jordan, T. E., Kana, T. M., Lang, M. W., 2014.
575 Searching for the missing nitrogen: biogenic nitrogen gases in groundwater and streams. J.
576 Agric. Sci., 152(S1), 96-106.

577 Gardner, J. R., Fisher, T. R., Jordan, T. E., Knee, K. L., 2016. Balancing watershed nitrogen
578 budgets: accounting for biogenic gases in streams. Biogeochemistry, 127(2-3), 231-253.

579 Gilbert, N. 2012. One-third of our greenhouse gas emissions come from agriculture. *Nature*.
580 News, 31 October 2012. *doi: 10.1038/nature.2012.11708.*

581 Glavan, M., Jamšek, A., Pintar, M., 2017. Modelling Impact of Adjusted Agricultural
582 Practices on Nitrogen Leaching to Groundwater. In Water Quality. InTech

583 Hasegawa, K., Hanaki, K., Matsuo, T., Hidaka, S., 2000. Nitrous oxide from the agricultural
584 water system contaminated with high nitrogen. Chemosphere-Global Change Science, *2*(3),
585 335-345.

586 Hinshaw, S. E., Dahlgren, R. A., 2016. Nitrous oxide fluxes and dissolved N gases (N_2 and
587 N_2O) within riparian zones along the agriculturally impacted San Joaquin River. Nutr. Cycl.
588 Agroecosys., 105(2), 85-102.

589 Hiscock, K. M., Bateman, A. S., Mühlherr, I. H., Fukada, T., Dennis, P. F., 2003. Indirect
590 emissions of nitrous oxide from regional aquifers in the United Kingdom. Environmental
591 science & technology, 37(16), 3507-3512

592 Hotchkiss, E. R., Hall Jr, R. O., Sponseller, R. A., Butman, D., Klaminder, J., Laudon, H.,
593 Rosvall, M., Karlsson, J., 2015. Sources of and processes controlling CO2 emissions change
594 with the size of streams and rivers. Nature Geoscience, 8(9), 696-699.

595 IPCC, 2014: Climate Change 2014: Synthesis Report. Contribution of Working Groups I, II
596 and III to the Fifth Assessment Report of the Intergovernmental Panel on Climate Change
597 [Core Writing Team, R.K. Pachauri and L.A. Meyer (eds.)]. IPCC, Geneva, Switzerland, 151
598 pp.

599 IPCC, 2006. In: Eggleston, H.A., Buendia, L., Miwa, K., Ngara, T., Tanabe, K. (eds). IPCC
600 guidelines for national greenhouse gas inventories. Prepared by the national greenhouse gas
601 inventories programme. IGES, Japan.

602 Jahangir, M.M., Johnston, P., Barrett, M., Khalil, M.I., Groffman, P.M., Boeckx, P., Fenton
603 O., Murphy, J., Richards, K.G., 2013. Denitrification and indirect N_2O emissions in
604 groundwater: hydrologic and biogeochemical influences. J. Contam. Hydrol., 152, 70-81.

605 Jahangir, M. M., Johnston, P., Khalil, M. I., Hennessy, D., Humphreys, J., Fenton, O.,
606 Richards, K. G., 2012. Groundwater: A pathway for terrestrial C and N losses and indirect
607 greenhouse gas emissions. Agr. Ecosys. Environ., 159, 40-48.

608 Johnson, M.S., Lehmann, J., Riha, S., Krusche, A.V., Richey, J.E., Ometto, J.P.H.B., Couto,
609 E.G., 2008. CO_2 efflux from Amazonian headwater streams represents a significant fate for
610 deep soil respiration. Geophys Res Lett 35:L17401.

611 Jurado, A., Borges, A.V., Pujades, E., Hakoun, V., Otten, J., Knoeller, K., Brouyère, S.,
612 2018. Occurrence of greenhouse gases in the aquifers of the Walloon Region (Belgium). Sci.
613 Total Environ., 619–620, 1579-1588.

614 Kendall, C., 1998. Tracing sources and cycling of nitrate in catchments. In: Kendall, C.,
615 McDonnell, J.J. (Eds.), Isotope Tracers in Catchment Hydrology. Elsevier, Amsterdam,
616 pp.519–576.

617 Kroopnick, P., Craig, H. (1972). Atmospheric oxygen: isotopic composition and solubility
618 fractionation. Science, 175(4017), 54-55.

619 Mayer, B., 2005. Assessing sources and transformations of sulphate and nitrate in the
620 hydrosphere using isotope techniques. In *Isotopes in the Water Cycle* (pp. 67-89). Springer
621 Netherlands.

622 Mayer, B., Bollwerk, S. M., Mansfeldt, T., Hütter, B., Veizer, J., 2001. The oxygen isotope
623 composition of nitrate generated by nitrification in acid forest floors. Geochimica et
624 Cosmochimica Acta, 65(16), 2743-2756.

625 McAleer, E. B., Coxon, C. E., Richards, K. G., Jahangir, M. M. R., Grant, J., Mellander, P.
626 E., 2017. Groundwater nitrate reduction versus dissolved gas production: A tale of two
627 catchments. Sci. Total Environ., 586, 372-389.

628 Minamikawa, K., Nishimura, S., Sawamoto, T., Nakajima, Y., Yagi, K., 2010. Annual
629 emissions of dissolved CO2, CH4, and N2O in the subsurface drainage from three cropping
630 systems. Global change biology, 16(2), 796-809.

631 Nikolenko, O., Jurado, A., Borges, A. V., Knöller, K., Brouyère, S., 2018. Isotopic
632 composition of nitrogen species in groundwater under agricultural areas: A review. Sci. Total
633 Environ., 621, 1415-1432.

634 Otero, N., Torrentó, C., Soler, A., Menció, A., Mas-Pla, J.,2009. Monitoring groundwater
635 nitrate attenuation in a regional system coupling hydrogeology with multi-isotopic methods:
636 the case of Plana de Vic (Osona, Spain). Agriculture, ecosystems & environment, 133(1),
637 103-113.

638 Raymond, P. A., Zappa, C. J., Butman, D., Bott, T. L., Potter, J., Mulholland, P., Laursen,
639 A.E., McDowell, W.H., Newbold, D., 2012. Scaling the gas transfer velocity and hydraulic
640 geometry in streams and small rivers. Limnology and Oceanography: Fluids and
641 Environments, 2(1), 41-53.

642 Rivett, M.O., Buss, S.R., Morgan, P., Smith, J.W.N., Bemment, C.D., 2008. Nitrate
643 attenuation in groundwater: A review of biogeochemical controlling processes. Water Res.,
644 42(16), 4215–4232.

645 SPW, DGARNE, 2010. État des lieux de la masse d'eau souterraine RWM021 « Calcaires et
646 Grès du Condroz ».

647 Sigman, D. M., Casciotti, K. L., Andreani, M., Barford, C., Galanter, M., Böhlke, J. K.,
648 2001. A Bacterial Method for the Nitrogen Isotopic Analysis of Nitrate in Seawater and
649 Freshwater." Analytical Chemistry 73(17): 4145-4153.

650 Tan, K. H.,2010. *Principles of soil chemistry*. CRC press.

651 Vidon, P., Serchan, S., 2016. Impact of stream geomorphology on greenhouse gas
652 concentration in a New York mountain stream. Water, Air, & Soil Pollution, 227(12), 428.

Vilain, G., Garnier, J., Tallec, G., Tournebize, J., 2012. Indirect N2O emissions from shallow groundwater in an agricultural catchment (Seine Basin, France). Biogeochemistry, 111(1-3), 253-271.

von der Heide, C., Böttcher, J., Deurer, M., Duijnisveld, W. H., Weymann, D., Well, R., 2009. Estimation of indirect nitrous oxide emissions from a shallow aquifer in northern Germany. J. Environ. Qual., 38(6), 2161-2171.

Wang, S., Yeager, K. M., Wan, G., Liu, C. Q., Liu, F., Lü, Y., 2015. Dynamics of CO2 in a karst catchment in the southwestern plateau, China. *Environmental Earth Sciences*, *73*(5), 2415-2427.

Wanninkhof, R., 1992. Relationship between wind speed and gas exchange over the ocean. J. Geophys. Res. 97, 7373-7382.

Werner, S. F., Browne, B. A., Driscoll, C. T., 2012. Three-dimensional spatial patterns of trace gas concentrations in baseflow-dominated agricultural streams: implications for surface–ground water interactions and biogeochemistry. Biogeochemistry, 107(1-3), 319-338.

Worral, F., Lancaster, A., 2005. The release of CO2 from river waters—the contribution of excess CO2 from groundwater. Biogeochemistry 76, 299–317.

675 **Figure captions**

676 **Figure 1.** Location and main aquifers of the Triffoy River catchment (Belgium). NL= The
677 Netherlands, LU=Luxemburg, DE=Germany, FR= France.

678 **Figure 2. (a)** Daily rainfall (mm), **(b)** air, river water and groundwater temperature and **(c)**
679 water level (m.a.s.l) of the river water in MPZ sampling location and of groundwater at
680 observation points MP2-6, MP3-6 and MP-4. Daily rainfall (mm) was measured by the
681 Walloon Public Service at Modave station.

682 **Figure 3.** Average concentrations for major ions, redox indicators, metals and greenhouse
683 gases in the Triffoy River and in the aquifer.

684 **Figure 4.** Spatial and temporal distribution of some major ions, redox indicators and
685 greenhouse gases in river water (SW) and groundwater (GW) for the samplings campaigns
686 carried out in December 2016 (a, b) and March 2017 (c, d). Note that the name of the
687 sampling points is on top of the x-axis.

688 **Figure 5.** $\delta^{15}N$ versus $\delta^{18}O$ values of nitrate for river water (grey dots) and groundwater
689 (black dots). The isotopic composition for the nitrate sources are taken from Kendall (1998)
690 and Mayer (2005).

691 **Figure 6.** Flux (E) of N_2O, CO_2 and CH_4 from the aquifer to the river (E_{gw}) and from the river
692 to the atmosphere (E_{riv}) from October 2016 to May 2017. Fluxes are expressed in kg Ha^{-1} y^{-1}
693 (per surface of river). Note the logarithmic scale for CH_4 fluxes.

694 **Table captions**

695 **Table 1.** Range and mean groundwater (7 observation points including MP-4, MP3-6, MP3-3,
696 MP2-6, MP2-3, S1 and S2) and river water (3 sampling locations named as Jamagne, MPZ
697 and State) concentrations for some major ions (mg/L), greenhouse gases (µg/L, ppm) and in-
698 situ parameters in the Triffoy River basin.

699

700

Figure 1.

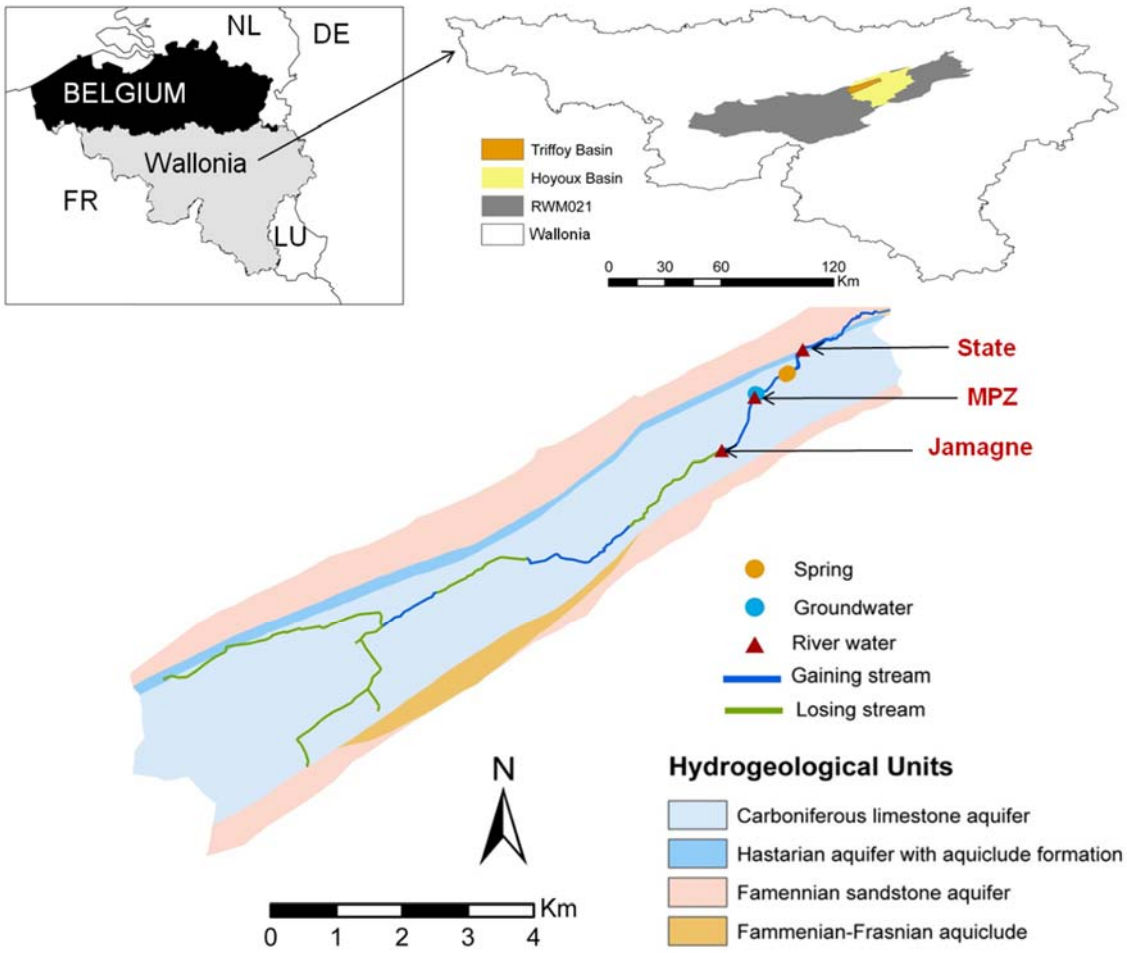
NL
DE
BELGIUM
Wallonia
FR
LU
Triffoy Basin
Hoyoux Basin
RWM021
Wallonia
0 30 60 120
Km
State
MPZ
Jamagne
Spring
Groundwater
River water
Gaining stream
Losing stream
N
0 1 2 3 4
Km
Hydrogeological Units
Carboniferous limestone aquifer
Hastarian aquifer with aquiclude formation
Famennian sandstone aquifer
Fammenian-Frasnian aquiclude

Figure 2.

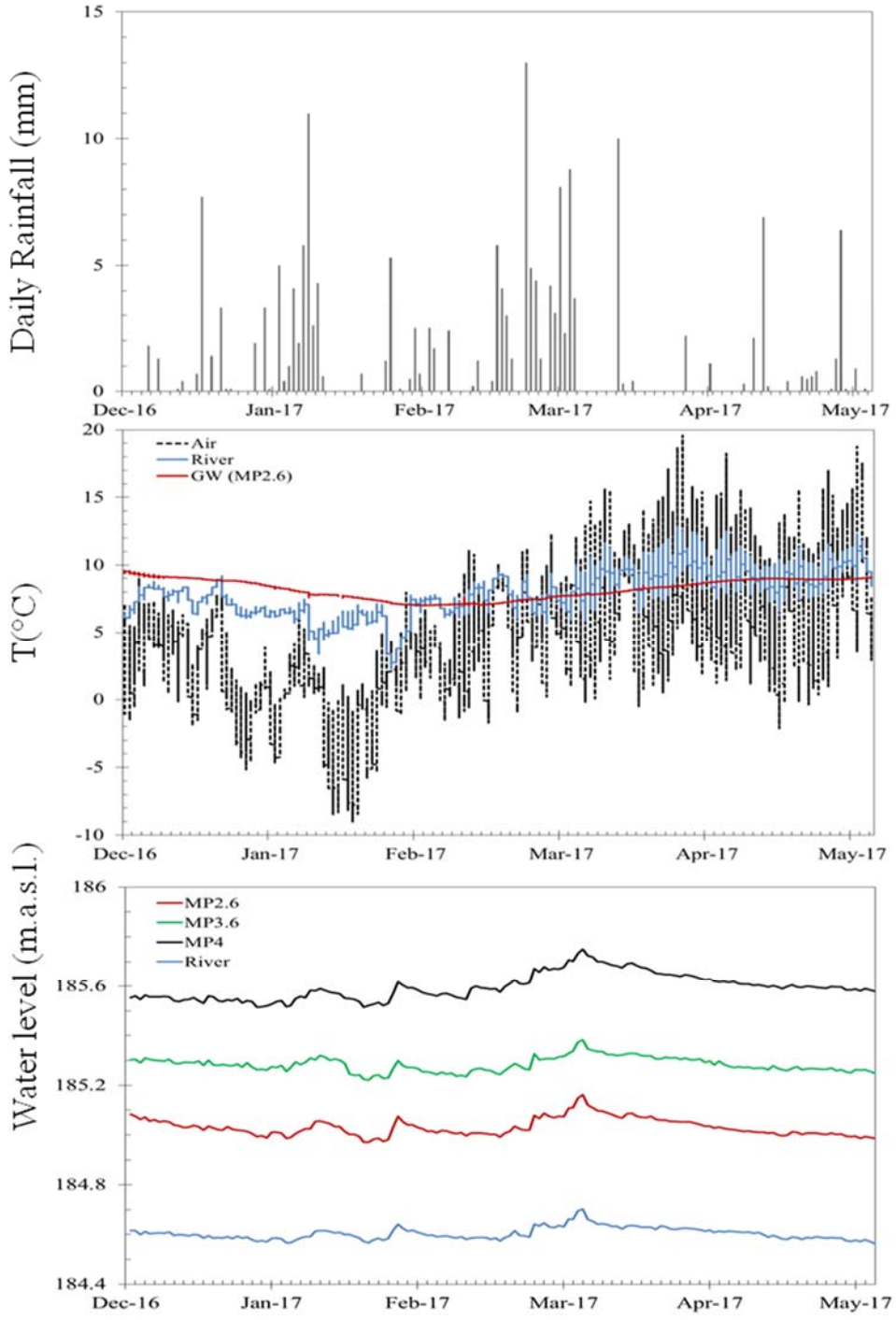
Daily Rainfall (mm)
15
10
5
0
Dec-16
Jan-17
Feb-17
Mar-17
Apr-17
May-17
T(°C)
Air
River
GW (MP2.6)
20
15
10
5
0
-5
-10
Water level (m.a.s.l.)
MP2.6
MP3.6
MP4
River
186
185.6
185.2
184.8
184.4

Figure 3

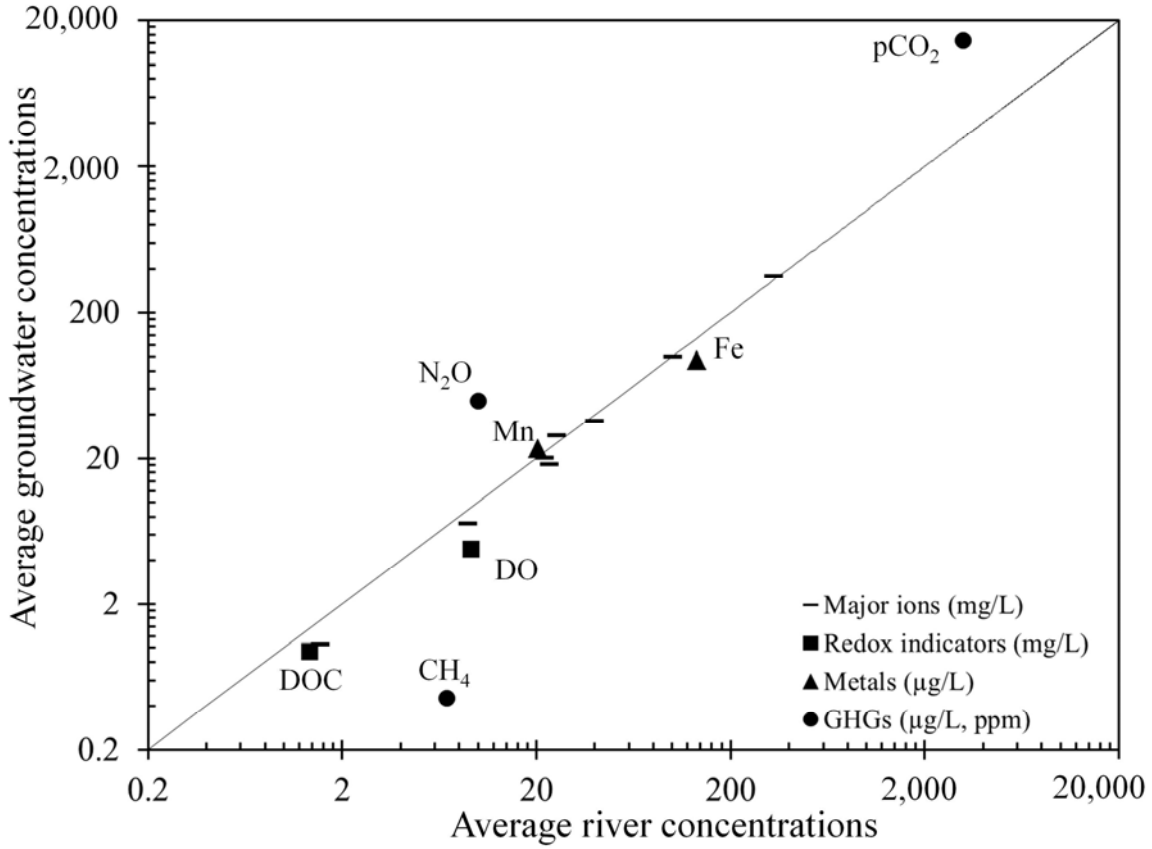
20,000
2,000
200
20
2
0.2
Average groundwater concentrations
0.2
2
20
200
2,000
20,000
Average river concentrations
pCO2
Fe
N2O
Mn
DO
DOC
CH4
Major ions (mg/L)
Redox indicators (mg/L)
Metals (µg/L)
GHGs (µg/L, ppm)

Figure 4.

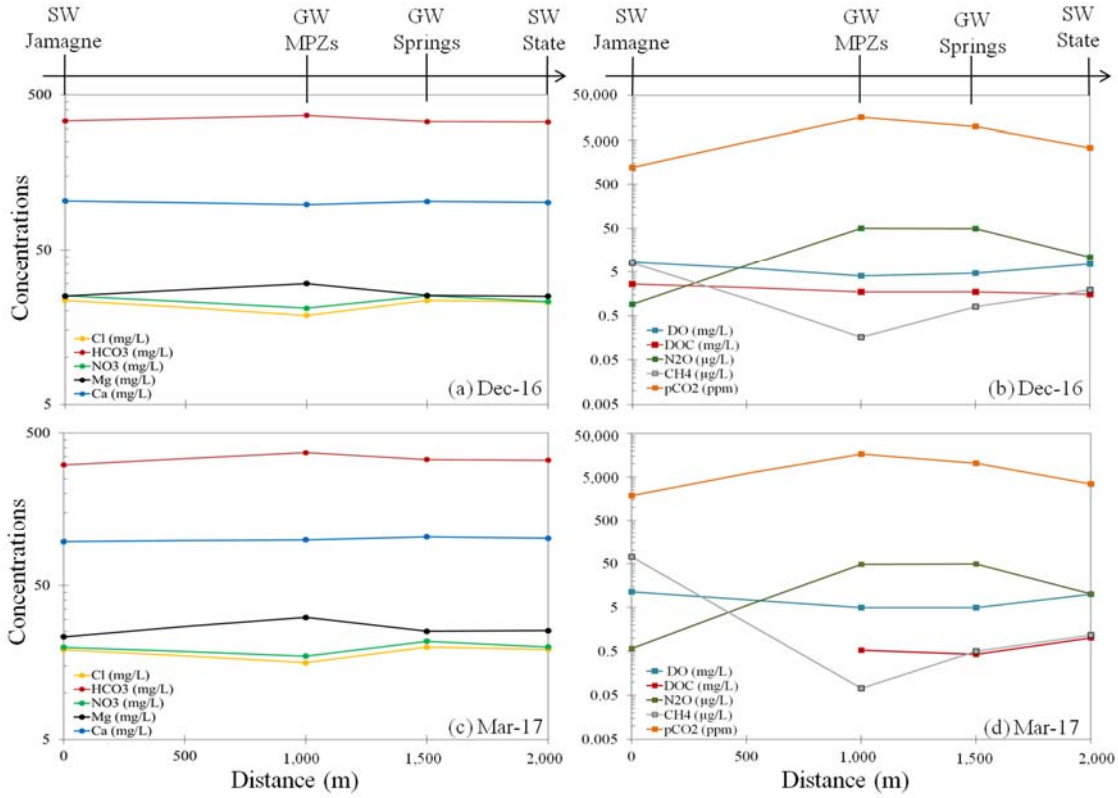
SW Jamagne
GW MPZs
GW Springs
SW State
Concentrations
Cl (mg/L)
HCO3 (mg/L)
NO3 (mg/L)
Mg (mg/L)
Ca (mg/L)
(a) Dec-16
DO (mg/L)
DOC (mg/L)
N2O (µg/L)
CH4 (µg/L)
pCO2 (ppm)
(b) Dec-16
(c) Mar-17
(d) Mar-17
Distance (m)

Figure 5

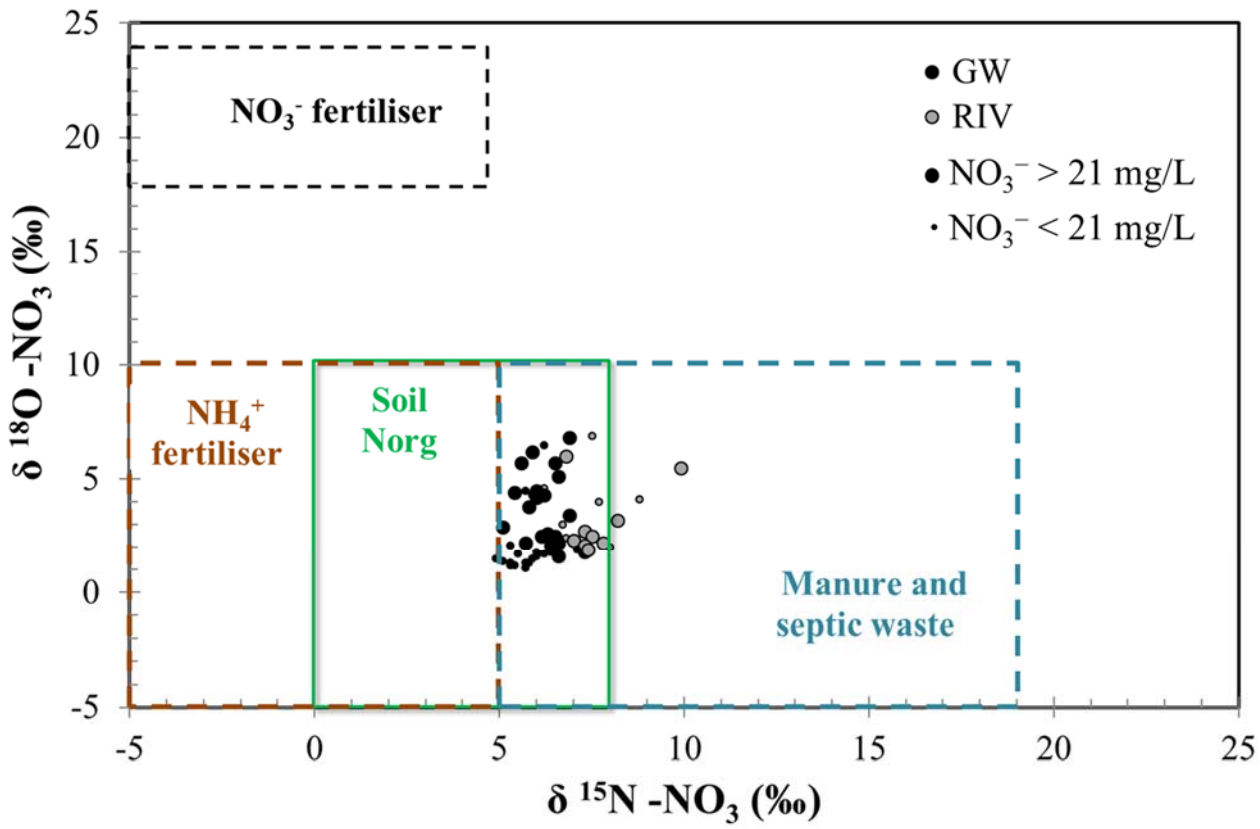
NO_3^- fertiliser
NH_4^+ fertiliser
Soil Norg
Manure and septic waste
GW
RIV
$NO_3^- > 21$ mg/L
$NO_3^- < 21$ mg/L
$\delta^{18}O$ -NO_3 (‰)
$\delta^{15}N$ -NO_3 (‰)
25
20
15
10
5
0
-5
-5
0
5
10
15
20
25

Figure 6

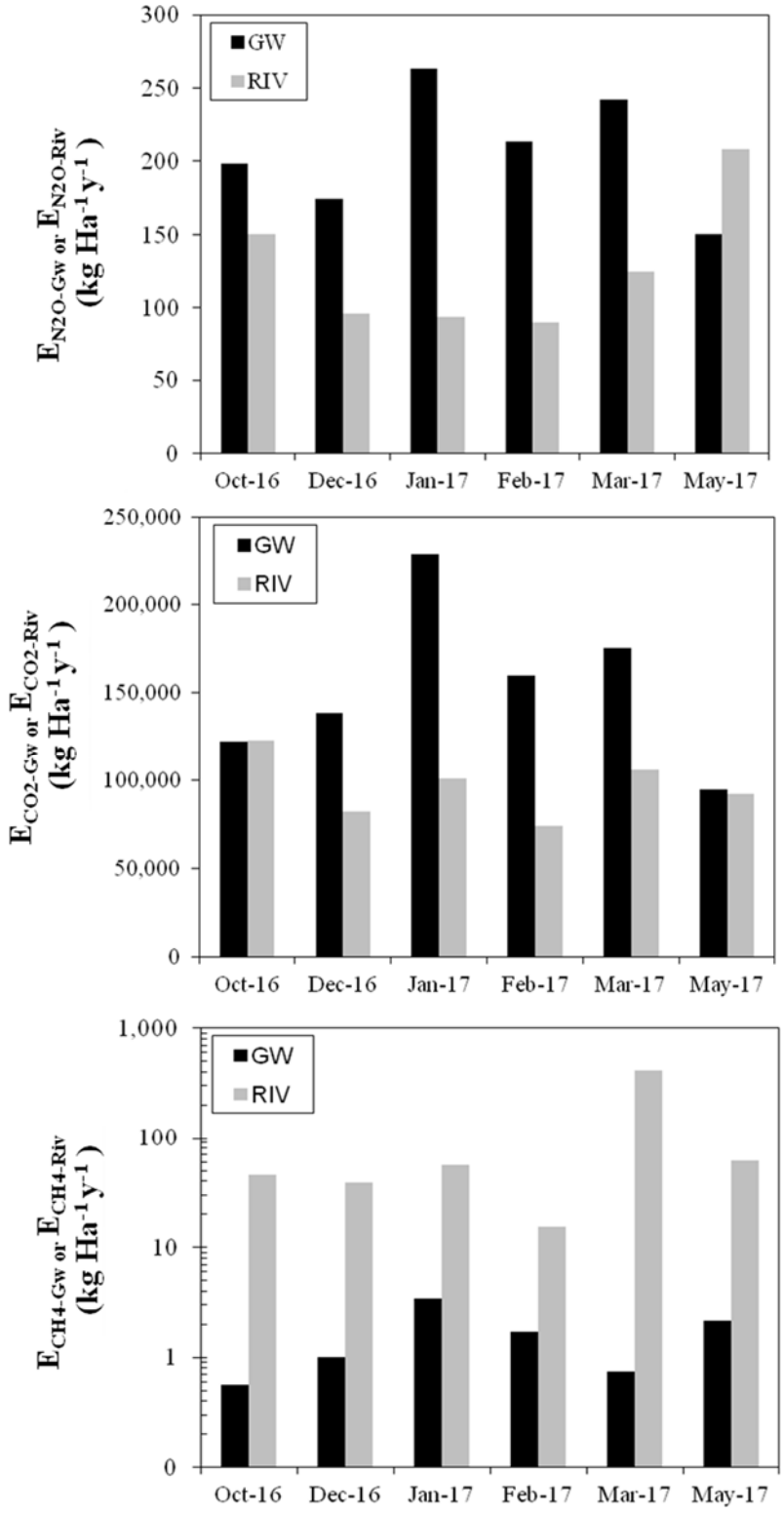
GW
RIV
$E_{N2O\text{-}Gw}$ or $E_{N2O\text{-}Riv}$ (kg Ha^{-1}y^{-1})
300
250
200
150
100
50
0
Oct-16
Dec-16
Jan-17
Feb-17
Mar-17
May-17
GW
RIV
$E_{CO2\text{-}Gw}$ or $E_{CO2\text{-}Riv}$ (kg Ha^{-1}y^{-1})
250,000
200,000
150,000
100,000
50,000
0
Oct-16
Dec-16
Jan-17
Feb-17
Mar-17
May-17
GW
RIV
$E_{CH4\text{-}Gw}$ or $E_{CH4\text{-}Riv}$ (kg Ha^{-1}y^{-1})
1,000
100
10
1
0
Oct-16
Dec-16
Jan-17
Feb-17
Mar-17
May-17

Table 1.

	HCO_3^- (mg/L)	Ca^{2+} (mg/L)	Mg^{2+} (mg/L)	NO_3^- (mg/L)	N_2O (µg/L)	CH_4 (µg/L)	pCO_2 (ppm)	DOC (mg/L)	DO (mg/L)	T (°C)	pH
MP-4	377.2-399.2 (384.3±8)	94.4-98.8 (97±1.5)	31.3-32.8 (32±0.64)	14.8-19.2 (16.9±1.9)	30.9-41.3 (35±4)	0.07-0.16 (0.10±0.04)	17,659-19,530 (18,312±667)	0.47-2 (0.98±0.59)	4.1-6.2 (5.3±0.95)	6.5-12 (10.2±1.9)	7.1-7.7 (7.4±0.21)
MP3-6	338.1-343 (340.1±1.7)	96.8-97.6 (97.2±0.26)	28.1-29.5 (28.7±0.59)	20.84-24.1 (22.3±1.2)	71.8-87.6 (79.1±5.2)	0.02-0.19 (0.09±0.06)	12,004-13,437 (12,793±582)	0.39-1.5 (0.90±0.46)	3.9-7.2 (4.7±1.2)	7.4-10.8 (10.1±1.4)	7-7.7 (7.4±0.22)
MP3-3	350.2-356.3 (353.6±2.2)	97.8-98.3 (98.1±0.26)	29.5-31.4 (30.1±0.79)	19.9-22.9 (21±1.1)	55.3-71.5 (61.6±6.1)	0.01-0.22 (0.11±0.09)	13,137-15,066 (14,107±784)	0.45-1.7 (0.91±0.52)	4.3-4.7 (4.5±0.19)	7.8-10.6 (9.6±1.3)	7.2-7.7 (7.4±0.21)
MP2-6	371.1-381.9 (374.9±4.4)	98.5-99.3 (98.7±0.28)	29.6-31.4 (30.7±0.63)	16.7-21.2 (19.1±1.7)	37.7-46.7 (43.5±3.1)	0.1-0.18 (0.15±0.03)	15,594-18,539 (17,365±1,164)	0.57-1.6 (1.1±0.43)	3.7-7.9 (5.1±1.5)	7-10.8 (9.6±1.5)	7-7.7 (7.4±0.26)
MP2-3	385.8-393.2 (391±3)	99.7-100.6 (100.2±0.33)	30.6-31.6 (31.2±0.41)	14.2-16.4 (15.6±0.89)	26-34.1 (30.9±3.1)	0.12-2.61 (0.98±1.1)	19,020-21,897 (20,000±1,138)	0.56-1.9 (1.1±0.50)	3.3-5.5 (4.3±0.79)	7-10.5 (8.8±1.4)	7.3-7.7 (7.3±0.28)
S1	336.4-331.6 (334.5±1.8)	102.8-103.6 (103.2±0.28)	24.3-25.2 (24.8±0.27)	21.4-24.7 (22.9±1.3)	34.5-44.4 (39.5±3.9)	0.64-4.8 (1.7±1.6)	9,353-8,285 (8,833±400)	0.37-1.9 (0.87±0.57)	4.7-6.2 (5.3±0.63)	8.3-10.7 (9.7±0.9)	7.1-7.8 (7.5±0.29)
S2	334.2-337.9 (336±1.4)	102.6-103 (102.7±0.17)	25.1-26.1 (25.5±0.36)	22-25.2 (23.4±1.4)	58.1-63.9 (59.5±2.2)	0.03-0.14 (0.10±0.04)	11,023-11,965 (11,399±343)	0.50-1.6 (0.80±0.45)	3.2-5.1 (4±0.63)	9.3-10.1 (9.8±0.38)	7.4-7.8 (7.5±0.15)
JAMAGNE	292.9-382.2 (326.5±32.3)	85.8-119 (100.2±11.3)	23.2-29.2 (24.8±2.3)	15.5-29.6 (22.3±4.8)	0.58-19.5 (7.6±4.1)	3-71.5 (18.9±26)	859-2,081 (1,612±488)	1.3-2.8 (2.1±0.70)	8.1-11.3 (9.3±1.40)	0.45-12.9 (6.6±5.2)	7.6-8.5 (8.2±0.34)
MPZ	330.8-349.1 (337±7.5)	97.3-105.1 (100.9±2.8)	24.6-27.2 (25.7±1)	19.8-25.2 (22.2±2.3)	12.8-18 (15.1±2.1)	0.28-0.65 (0.42±0.13)	3,812-4,975 (4,390±459)	0.7-2.2 (1.3±0.60)	8-10 (9.2±0.78)	5.9-10.1 (7.9±1.8)	7.8-8 (7.9±0.09)
STATE	332-338.2 (334.3±2.3)	100.1-102.5 (101.3±0.86)	24.8-26.5 (25.4±0.57)	19.8-22.9 (21.5±1.3)	9.7-12.4 (10.9±1)	0.86-2.1 (1.4±0.48)	3,281-3,973 (3,502±253)	0.6-1.5 (94±0.34)	7.5-11.1 (9±1.3)	7.1-11.3 (9.3±1.8)	7.8-8.1 (7.9±0.10)